

# REDUCTION OF FALSE POSITIVE DETECTION IN CLUSTERED MICROCALCIFICATIONS

Juan Wang, Yongyi Yang, and Robert M. Nishikawa<sup>1</sup>

Department of Electrical and Computer Engineering, Illinois Institute of Technology, Chicago, IL 60616

<sup>1</sup>Department of Radiology, The University of Chicago, Chicago, IL 60637

## ABSTRACT

Linear structures are a major source of false positives (FPs) in computer-aided detection of clustered microcalcifications (MCs) in mammograms. In this work, we investigate whether it is feasible to improve the performance in MC detection by directly exploiting the FPs associated with linear structures. We analyze the cause of FPs by linear structures and their characteristics with an SVM detector, and design a linear structure detection procedure together with a dual-thresholding scheme to separate the linear structures from other tissue background in a mammogram. The proposed procedure was demonstrated on a set of 200 mammograms containing clustered MCs. The results show that it could effectively reduce the FPs in the SVM detector by as much as 30% with the true detection rate at 85%.

**Index Terms**— Computer-aided diagnosis (CAD), linear structure detection, false positive reduction.

## 1. INTRODUCTION

Microcalcifications (MCs) are tiny calcium deposits which appear as bright spots in mammograms (e.g. Fig. 1(a)). Clustered MCs are found in 30-50% of mammographically diagnosed cases, and they can be an important early sign of breast cancer in women. However, MCs can be difficult to detect because of their subtlety in appearance, variation in shape and size, and the surrounding breast tissue [1]. Because of its importance in early diagnosis, there have been great efforts in development of computer-aided diagnosis (CAD) algorithms for MC detection and classification [2], which has led to several FDA approved commercial CAD systems.

Despite these efforts, however, the performance of existing CAD algorithms for MC detection is still far from being perfect. One often cited factor in degrading performance is the frequent occurrence of false-positives (FPs) when the true-positive (TP) rate is at a reasonable detection level. In MC detection, the FPs can be caused by a number of factors, including imaging noise, inhomogeneity in tissue background, artifacts and linear structures.

In the literature there have been several studies toward reduction of FPs in MC detection. In [3] Ema *et al* grouped FPs into four categories and extracted image features on

local edge gradients and the degree of linearity to eliminate FPs using a thresholding scheme. Subsequently, Bazzani *et al* [4] used an SVM classifier on similar image gradient and linearity features to remove FPs. Chen and Zhao [5] proposed use of RANSAC feature along with other features to remove FPs caused by linear structures.

Linear structures in mammograms can be attributed to various sources including vessels, ducts, fibrous tissue, skinfolds, edges and other anatomical features [6]. They are found to be a major cause of FPs in previously developed CAD algorithms. For example, Ema *et al* [3] reported that as high as 22.8% of the FPs were caused by linear structures from an analysis of 311 FPs in 39 mammograms. It is expected that the accuracy in detecting clustered MCs in mammograms will be significantly improved by effectively reducing FPs caused by linear structures.

In this work, our goal is to investigate whether it is feasible to improve the overall performance in MC detection by directly exploiting the FPs associated with linear structures in mammograms. In particular, we will develop our approach by making use of an SVM detector for MC developed in [7], which was demonstrated to yield more robust detection in performance (higher TP rate and lower FPs) when compared to several representative methods in the field. While we demonstrate our approach using this SVM detector, in principle it can be applied to other MC detectors as well, e.g., the difference of Gaussian detector [8].

Conceptually, to avoid FPs caused by linear structures, a seemingly straightforward approach would be to first apply an (optimal) detection algorithm to remove the linear structures altogether in a mammogram prior to MC detection. However, as explained in detail later, such an approach is compromised by the fact that MCs can overlap with linear structures in a mammogram and that closely distributed MCs in a cluster can be mis-detected as linear structures. Consequently, such an approach would adversely result in false-negatives in the detection.

In this work, we will analyze the main cause of FPs by linear structures and their characteristics in the detector output, and develop a strategy to suppress the FPs accordingly. We employ a linear structure detection procedure to identify those image pixels on linear structures,

---

This work was supported by NIH/NIBIB grant R01EB009905.

and process them separately from other tissue background. The advantage of such approach is that it separates the task of MC detection from that of linear structures, thereby avoiding the need to retrain the SVM detector by introducing some additional edge or linearity related image features. As we demonstrate in the experiments, while computationally simple, such approach can effectively reduce the FPs in the SVM detector by as much as 30% when the TP rate is at 85%.

It is noted that there have been several algorithms proposed in the literature for the purpose of detecting abnormal tissue structures in mammograms. Zwiggelaar *et al* [9] compared four linear structure detection algorithms for classifying anatomical tissue types and concluded that the line operator in [10] had the best performance. Berks *et al* [11] applied random forest classification on wavelet features for determining abnormal linear structures in mammograms. Bator and Chmielewski [12] applied an accumulation-based line detector for decreasing FPs in cancerous mass detection. To our best knowledge, none of these studies directly deal with removing FPs associated with linear structures in MC detection.

## 2. METHODS

### 2.1 Motivation of the problem

Because of the spatially localized nature of MCs in a mammogram image, most of the MC detectors, if not all, rely on use of image features such as contrast and edge gradient derived locally around the detection location. When examined locally, a small segment of a linear structure would lead to similar image features of an MC (e.g., high contrast and image gradient), thereby causing false detection by the MC detector.

To illustrate this, in Fig. 1(a) we show two mammogram ROIs which contain both MCs and line structures; in Fig. 1(b) we show their corresponding detection output obtained by an SVM detector [7]. As can be seen, while the detector has correctly located most of the MCs, it has also led to a number of FPs along the linear structures. These FPs would be falsely treated as clustered MCs when they occur in close vicinity of each other.

In view that the MC detector output has different characteristics in linear structures from that in other tissue background, we propose to apply a detection algorithm to first identify the linear structures in a mammogram image which will be treated separately from the rest of the image in the detector output.

### 2.2 Linear structure detection

Below we develop our detection procedure by making use of an existing line detector in the literature. In particular, we will use the line operator in [10] which was demonstrated to be effective for detecting linear structures in mammograms [9].

#### *a) Issues with line detection in presence of MCs*

The line operator in [10] is based on directional template-matching with different orientation angles. Specifically, for a given image, a line strength signal  $S(\mathbf{x})$  is first computed at each pixel location  $\mathbf{x}$  as:

$$S(\mathbf{x}) = L(\mathbf{x}) - N(\mathbf{x}), \quad (1)$$

where  $N(\mathbf{x})$  is the local background intensity around  $\mathbf{x}$  and  $L(\mathbf{x})$  is the output of the directional line-template which is obtained as:

$$L(\mathbf{x}) = \max_{\theta_i \in \{0, \pi\}} L_{\theta_i}(\mathbf{x}), \quad (2)$$

where  $L_{\theta_i}(\mathbf{x})$  denotes the template output at orientation  $\theta_i$ . For a linear structure, the template detector  $L_{\theta_i}(\cdot)$  yields its maximum output when its orientation is in perfect alignment with the linear structure. The line strength signal  $S(\mathbf{x})$  is compared against a threshold  $T_l$  to obtain a binary map of the detected linear structures.

While computationally simple, we find that this line operator suffers from some drawbacks when applied directly for the task of MC detection. Specifically, 1) owing to the high intensity values of MCs, the detector output at a linear structure can be greatly affected by the presence of MCs in its vicinity; 2) when several MCs are densely distributed in a cluster, they will cause the detector to have high output values, leading to misdetection of these MCs as a linear structure; 3) the detector will miss detection at locations when two linear structures intersect or when a linear structure splits into two. These locations happen to likely lead to FPs in the MC detector owing to their similarity to MCs.

#### *b) Modified line detection procedure*

To deal with the above issues, we adapt the line operator for the purpose of MC detection by including the following two major components: 1) weighted directional template, and 2) post-processing.

1) *Weighted directional template.* Different from [10], the weight coefficients in the directional template  $L_{\theta_i}(\cdot)$  are designed to be tapering off toward the both ends along the directional template. This is to mitigate the influence on the detector output when there are MCs in the vicinity of a linear structure (Issue #1 above). In our experiments, a Gaussian function (with standard deviation 5.2) was used for the weight coefficients of the template  $L_{\theta_i}(\cdot)$  along its orientation; also, the following parameters were used for the line template: length 21 pixels, width 3 pixels, and 12 equally-spaced orientation angles (i.e., resolution 15°). Such a choice was geared toward those linear structures having width similar to the dimension of an MC (the image resolution was 100  $\mu m$ ). In Fig. 2 we show the resulting template for several orientation angles.

2) *Post-processing of false detection.* To deal with the other two issues pointed out above (#2 and #3), the output of the line detector is subsequently processed with the following two steps: 1) direction dilation, and 2) false detection removal, which we describe below.

First, the detector output signal  $S(\mathbf{x})$  is observed to be reduced in magnitude near locations where two linear structures intersect or one linear structure splits into two, resulting in misdetection at these locations (Issue #3). To deal with this issue, we apply a morphological dilation to the detector output with a linear structural element along the direction of each detected linear segment. In our experiments, this structural element was chosen to be 1 pixel in width and 11 pixels in length (based on the typical width of an MC).

Next, it is observed that the strength signal  $S(\mathbf{x})$  gets increased near a cluster of densely distributed MCs, or along a group of linearly distributed MCs, which would result in these MCs being misclassified as a linear structure (Issue #2). To discriminate such false detections from linear structures, we analyzed the image features of false detections associated with MCs based on a training set of mammogram images (Sect. 3.1). Based on this analysis, we extract the following features for each detected segment with length less than 1 cm (out of the consideration that only those densely distributed MCs can affect the detector output): 1) compactness  $C = 4\pi A/P^2$ , where  $A$  and  $P$  denote the area and perimeter of the segment, respectively, 2) area to perimeter ratio  $R = A/P$ , and 3) standard variation  $\sigma_i$  of the image intensity within the segment. A detected segment will be removed if it meets one of the following three criteria:

- 1)  $C > 0.25$ ,
- 2)  $C \leq 0.25$  and  $R > 3$ , or
- 3)  $\sigma_i > 1.35\sigma_b$ , where  $\sigma_b$  is the standard deviation of the background.

The parameters in these criteria were determined based on the discriminant analysis of the false detections against the features of linear structures. Among them the first condition requires the detected segment to be sufficiently elongated to qualify as a linear structure; the second condition is to ensure that in the case of intersecting or splitting structures, the segment is predominantly linear in extent; the third condition is based on the fact that when multiple MCs are closely distributed in a detected segment, they will cause a significant increase in the variation of image intensity along the segment.

### 2.3 FP reduction by dual-thresholding

Upon analyzing the detector output  $f(\mathbf{x})$ , we observed that the statistical properties of  $f(\mathbf{x})$  at pixels in a linear structure are different from that of other tissue background. Specifically, the response in a linear structure is generally higher than in the background; the response at pixels where the MCs overlapping with a linear structure is also generally higher than at pixels in the linear structure; moreover, the FPs caused by a linear structure have higher response than the FPs caused by other tissue background.

Based on these observations, we adopt a dual thresholding scheme for the detector output in order to deal

with the linear structures separately from the rest of a mammogram image. First, for pixel locations not on a linear structure, we set the threshold as  $T_0 = \mu_0 + \alpha\sigma_0$ , where  $\mu_0$  and  $\sigma_0$  are the mean and standard deviation of the detector output  $f(\mathbf{x})$  estimated from all the tissue pixels in the image except for those at linear structures. The parameter  $\alpha$  is used to set the operating point of the detector. Next, for pixels in a detected linear structure, we set the threshold as  $T_1 = \mu_1 + \alpha\sigma_1$ , where  $\mu_1$  and  $\sigma_1$  are the mean and standard deviation of the detector output estimated from all the linear structures in the image.

## 3. EXPERIMENTS AND RESULTS

### 3.1 Mammogram dataset

We make use of a dataset collected by the Department of Radiology at the University of Chicago. It consists of a total of 200 mammogram images, all containing multiple MCs. These images are of dimension 1024×1024 or 512×512 pixels, digitized with a spatial resolution of 0.1 mm/pixel and 10-bit grayscale. The MCs in each mammogram were manually identified by a group of experienced radiologists. These MCs were used as the ground truth for evaluation.

Prior to MC detection, the mammogram images were first pre-processed by a high-pass filter for the purpose of suppressing the inhomogeneity of the tissue background in each mammogram [7]. Afterward, a noise equalization procedure [13] was applied for equalizing the intensity-dependent noise in the image.

The dataset was randomly partitioned into two subsets, one with 100 mammograms for training and the other with 100 mammograms for testing. The training mammogram images were used both for training the MC detector and for tuning the parameters in the linear structure detection procedure.

### 3.2 Performance evaluation

To demonstrate the effect of linear structures, we use the SVM classifier developed in [7] for MC detection. To evaluate the detection performance, we conduct a free-response receiver operating characteristic (FROC) analysis, which is now routinely used for performance evaluation in MC detection. An FROC curve is a plot of the correct detection rate of MC clusters (i.e., true positive fraction) versus the average number FPs per image with the decision threshold continuously varied over its operating range.

The detected objects by the MC detector were grouped into clusters using the criterion described in [14]. Specifically, a group of objects is considered to be a cluster if the objects are connected with nearest-neighbor distances less than 0.5 cm and there are at least three objects within a square area of 1 cm<sup>2</sup>. A detected cluster is considered as a TP cluster if: (1) it includes at least two true detected MCs; (2) its center of gravity is within 1 cm of that of a known true MC cluster. Likewise, a detected cluster is considered as a FP cluster provide that (1) it contains no true MCs, or (2)

the distance between its center of gravity and that of any known cluster is larger than 1 cm. It should be noted that the FROC curves can be sensitive to the detection criteria [7] and the results should be compared with caution when they were reported with different criteria in the literature.

To remove the effect of case distributions in the dataset, we adopted a bootstrapping procedure on the test set of mammograms for obtaining the FROC [15]. A total of 20,000 bootstrap samples were used, based on which the area under FROC curve (AUC) was obtained.

### 3.3 Results

In Fig. 3 we show the obtained FROC curve with the proposed linear structure detection procedure by the SVM detector; for comparison the results are also shown for the SVM detector without the proposed procedure (SVM baseline). As can be seen, the proposed procedure yields a higher FROC curve; a statistical comparison between the two yields a mean difference of 0.0888 in AUC ( $p$ -value=0.00015) for the FP rate in the range between 0.4 and 2 per image. Moreover, it achieved an average improvement of 5.32% in TPF for FP rate in the range between 0.8 and 1.4. For TPF at 85%, the number of FPs has been reduced from 1.4 to 1.05, nearly a 30% reduction.

In Fig. 1(c), we show the detection results by incorporating the proposed linear structure detection in the MC detector for the two sample ROIs in Fig. 1(a). Both ROIs have noticeable linear structures, of which the ROI on the left has a linear structure splitting into two, and the ROI on the right has MCs overlapping with linear structures. Compared with the SVM baseline in Fig. 1(b), the proposed FP reduction procedure has removed most of the FPs caused by the linear structures while still detecting most of the MCs in both cases.

## 4. CONCLUSION

We investigated the use of a linear structure detection procedure and a dual-thresholding scheme for reduction of FPs caused by linear structures in MC detection. The results show that it could significantly reduce the FPs caused by linear structures, thus improving the overall performance of MC detection. In future work it would be interesting to study how to extend it for FPs caused by other sources.

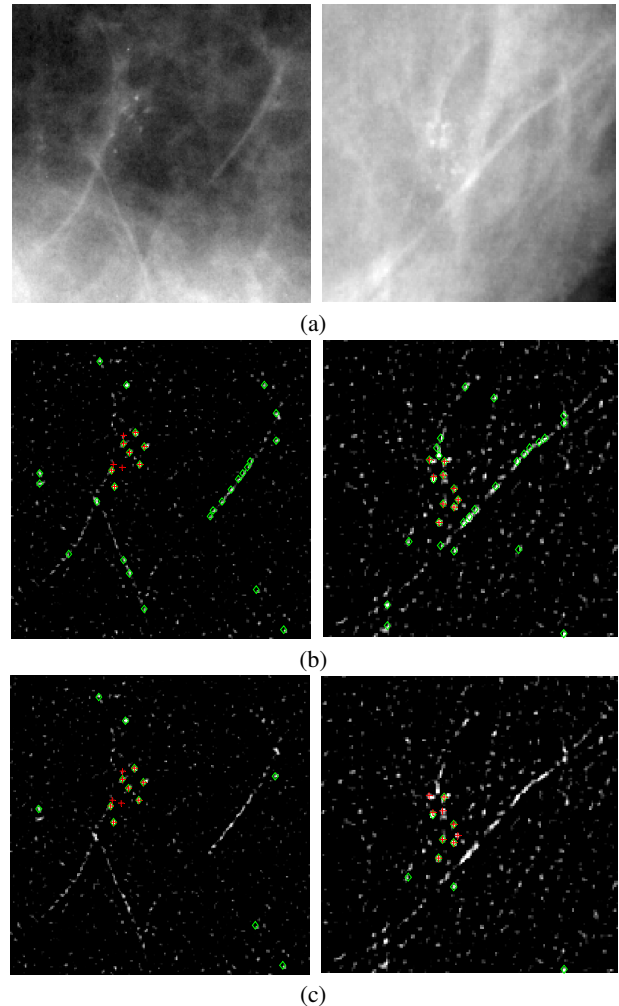


**Fig. 1.** (a) Two sample mammogram ROIs containing MCs; (b) output of MC detector on the two ROIs, wherein MCs are indicated by red '+' symbols, and detections are indicated by green diamond symbols; (c) MC detection results obtained with the proposed linear structure detection procedure.

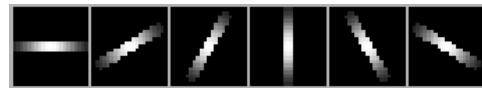


**Fig. 2.** Examples of directional template in orientations of 0°, 30°, 60°, 90° and 120°, and 150°, respectively.

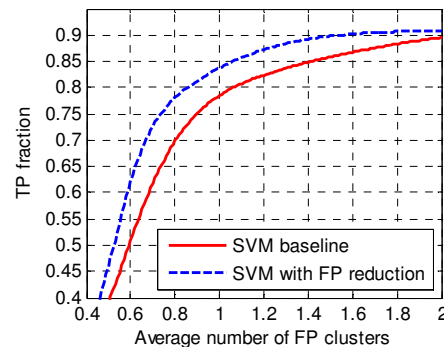


**Fig. 3.** FROC curves obtained with and without linear structure detection based on 20,000 bootstrap samples.

## 5. REFERENCES

- [1] M. Lanyi, "Diagnosis and differential diagnosis of breast calcifications," Berlin, Germany: Springer-Verlag, 1988.
- [2] K. Thangavel, M. Karnan, *et al*, "Automatic detection of microcalcification in mammograms – A review," *ICGST International Journal on Graphics, Vision and Image Processing*, vol. 5, no. 5, 2005.
- [3] T. Ema, K. Doi, *et al*, "Image feature analysis and computer-aided diagnosis in mammography: Reduction of false-positive clustered microcalcifications using local edge-gradient analysis," *Med. Phys.*, vol. 22, 1995.
- [4] A. Bazzani, A. Bevilacqua, *et al*, "An SVM classifier to separate false signals from microcalcifications in digital mammograms," *Phys. Med. Biol.*, vol. 46, 2001.
- [5] S. Chen and H. Zhao, "False-positive reduction using RANSAC in mammography microcalcification detection," *Proc. of SPIE*, 2011.
- [6] R. Zwigelaar and C. R. M. Boggis, "The benefit of knowing your linear structures in mammographic images," *Proceedings of Medical Image Understanding and Analysis*, 2002.
- [7] I. El-Naqa, Y. Yang, M. N. Wernick, N. P. Galasanos, and R. M. Nishikawa, "A support vector machine approach for detection of microcalcifications," *IEEE Trans. Med. Imag.*, vol. 21, 2002.
- [8] J. Dengler, S. Behrens, and J. F. Desaga, "Segmentation of microcalcifications in mammograms," *IEEE Trans. Med. Imag.*, vol. 12, 1993.
- [9] R. Zwigelaar, S. M. Astley, C. R. M. Boggis, and C. J. Taylor, "Linear structures in mammographic images: detection and classification," *IEEE Trans. on Med. Imag.*, vol. 23, 2004.
- [10] R. N. Dixon and C. J. Taylor, "Automated asbestos fiber counting," *Machine Aided Image Analysis*, 1979.
- [11] M. Berks, Z. Chen, *et al*, "Detecting and classifying linear structures in mammograms using random forests," *Information Processing in Medical Imaging, LNCS 6801*, pp. 510-524, 2011.
- [12] M. Bator and L. J. Chmielewski, "Elimination of linear structures as an attempt to improve the specificity of cancerous mass detection in mammograms," *Computer Recognition systems 2, ASC 45*, 2007.
- [13] W. J. H. Veldkamp and N. Karssemeijer, "Normalization of local contrast in mammograms," *IEEE Trans. Med. Imag.*, vol. 19, 2000.
- [14] R. M. Nishikawa, "Current status and future directions of computer-aided diagnosis in mammography," *Comput. Med. Imaging Graph.*, vol. 31, 2007.
- [15] F. W. Samuelson and N. Petrick, "Comparing image detection algorithms using resampling," *Proc. Inter. Symp. on Biomedical Imaging: From Nano to Macro*, 2006.